Upstream Erosion and Sediment Passage at Piano Key Weirs

Mattia Noseda[1]; Ivan Stojnic[2]; Michael Pfister[3]; and Anton J. Schleiss, M.ASCE[4]

Abstract: Piano key weirs (PKWs) are a weir type characterized by an effective rating curve. Accordingly, this control structure is primarily applied at dams to increase the spillway capacity. In recent years, PKWs also have been implemented in rivers combined with low-head hydropower or to regulate waterways. For the latter application, a weir type without gates may be favorable, but the issue of the passage of sediments arises. Such sediments are either deposited in the backwater or transported to the weir during intense floods. An efficient sediment passage is necessary to avoid inundations upstream of the weir and to maintain a navigable waterway. Two options arise: (1) to flush the sediments (e.g., through a gate in the weir), or (2) to carry them over the weir crest. The second option is favorable, if upstream riverbed aggradation can be avoided, because no mechanical devices (i.e., gates) are used. This study analyzed the sediment passage over a PKW driven uniquely by the flow. Systematic physical model tests were conducted to study the upstream riverbed behavior as well as the passage of sediments over the PKW. Three PKW configurations, two sediment granulometries, and six discharges were considered. Key results refer to the modified rating curve under high riverbed levels and to the upstream scour process of sediment deposits. Finally, the sediment passage capacity was linked to the equilibrium sediment transport conditions upstream of a PKW. Pragmatically formulated, this relation indicates—at least for the tested configurations—that sediments arriving at the PKW also pass over it. **DOI: 10.1061/(ASCE)HY.1943-7900.0001616.**

Author keywords: Piano key weir; Rating curve; Riverbed; Sediment passage; Scour.

Introduction

Piano key weirs (PKWs) convey discharges with a comparable low upstream hydraulic head (Leite Ribeiro et al. 2012; Machiels et al. 2014). They require a relatively small construction footprint in the streamwise direction and provide passive discharge control. These aspects make PKWs an efficient inlet structure on top of a spillway. Thus, PKWs are mainly used to enhance the discharge capacity of existing spillways and as an inlet structure of newly constructed auxiliary spillways (Laugier et al. 2013; Phillips and Lesleighter 2013), both typically implemented on concrete gravity dams.

So far, only a few PKWs have been built as control structures in rivers (e.g., Van Phong in Vietnam and Giritale in Sri Lanka). Such applications imply particular issues (Belzner et al. 2016; Herbst et al. 2018; Oertel 2018), such as driftwood blockage and its influence on the rating curve (Pfister et al. 2013b; Venetz 2014), submerged operation (Dabling and Tullis 2012), downstream toe-scouring (Jüstrich et al. 2016), and sediment passage during floods (Gebhardt et al. 2018). The latter issue is relevant to avoid floodplain inundation because of sedimentation in the backwater, and also to keep rivers navigable and operational in terms of flood discharge capacity (Belzner et al. 2016, 2017).

Only a few studies have focused so far on the upstream erosion or sediment passage at weirs. Cassidy et al. (1985) investigated the effect of sediment depositions near the Boardman labyrinth, stating that the "deposition had negligible effect on the spillway rating." Falvey (2003) described the sedimentation characteristics referring to Boardman, Hellsgate, and Garland labyrinth weirs. He concluded that the related studies showed that labyrinth weirs are self-cleaning, meaning that sediments deposited during low flows are scoured under flood conditions. Lauchlan (2004) conducted model tests on bed-load transport over linear sharp-crested weirs, describing a strong down-flow vortex immediately upstream of the weir. This vortex induced scour at the weir front and lifted sediments so that they were transported in suspension over the weir. No sediment deposits were detected by Lauchlan upstream of the weir. Sharma and Tiwari (2013) measured flow velocities upstream of a model PKW. They recorded relatively strong vertical components near the upstream PKW front, even under low discharges, linking this to sediment suspension. Guan et al. (2015) experimentally investigated the scour process upstream and downstream of submerged linear sharp-crested weirs under live-bed conditions. Strong down-flows were observed at the upstream front of the weir. A scour-and-fill process occurred in response to periodic approaching bed forms. Under clear-water conditions, a small scour hole was observed at the upstream weir front. This hole was produced by vortices generated by the interaction of the approach flow and the local back flow. Sediment transport over the weir took place as suspended load.

Two test campaigns were conducted at the Federal Waterways Engineering and Research Institute (BAW), Germany, related to

[1]Civil Engineer, Laboratory of Hydraulic Constructions, Ecole Polytechnique Fédérale de Lausanne, Lausanne CH-1015, Switzerland; presently, Project Engineer, AF-Consult Switzerland, Täfernstrasse 26, Baden CH-5405, Switzerland.

[2]Laboratory of Hydraulic Constructions, Ecole Polytechnique Fédérale de Lausanne, Lausanne CH-1015, Switzerland; Ph.D. Student, Instituto Superior Técnico, Universidade de Lisboa, 1049-001 Lisbon, Portugal.

[3]Professor, Dept of Civil Engineering, Haute Ecole d'Ingénierie et d'Architecture de Fribourg (HEIA-FR, HES-SO), Fribourg CH-1705, Switzerland (corresponding author). Email: michael.pfister@hefr.ch

[4]Professor Emeritus, Laboratory of Hydraulic Constructions, Ecole Polytechnique Fédérale de Lausanne, Lausanne CH-1015, Switzerland.

Note. This manuscript was submitted on August 9, 2018; approved on January 18, 2019; published online on June 6, 2019. Discussion period open until November 6, 2019; separate discussions must be submitted for individual papers. This paper is part of the ***Journal of Hydraulic Engineering***, © ASCE, ISSN 0733-9429.

Table 1. Tested PKW configurations (model dimensions)

Configuration	A	B	C
W (m)	0.665	0.545	0.555
W_i (m)	0.040	0.082	0.044
W_o (m)	0.033	0.050	0.039
$W_u = W_i + W_o + 2T_s$ (m)	0.093	0.148	0.085
T_s (m)	0.010	0.008	0.001
B (m)	0.325	0.325	0.190
B_o (m)	0.100	0.118	0.055
B_i (m)	0.075	0.090	0.050
$P = P_i = P_o$ (m)	0.150	0.096	0.084
R (m)	0.020	0.000	0.017
L/W	7.80	5.20	5.50
W_i/W_o	1.21	1.64	1.13
B/P	2.17	3.39	2.26
B_i/B	0.23	0.28	0.26
B_o/B	0.31	0.36	0.29

labyrinth weirs and, among other things, sediments. Herbst (2016) studied labyrinth weirs with a trapezoidal or rectangular footprint (weir height $P = 0.255$ m), with three different granulometries ($d_s = 2.0$, 2.1, and 5.6 mm). A sediment ramp inside the weir and an upstream deposit were provided prior to a test. The discharge was then progressively increased until inception of sediment motion occurred, resulting in a bed bathymetry measured after 15 min of steady flow. A test ended as soon as the weir cycles were emptied and thus free of sediments. Herbst (2016) reported that the discharge of incipient sediment motion at the weir was at some 14%–27% of the upstream channel incipient discharge, suggesting that erosion starts at labyrinth weirs under much lower discharges than in the channel. Leitz (2016) completed the work of Herbst (2016) with a fourth granulometry ($d_s = 0.7$ mm), but focused exclusively on the self-cleaning capacity. Duration tests indicated that the erosion process is slower for fine sediments than for larger particles.

Ota et al. (2017) conducted numerical simulations and physical scour tests at a slit weir for steady and unsteady flows. They related the scour depth to the eroded volume and the relative slit width. Gebhardt et al. (2018) extended the model studies of Herbst (2016) and Leitz (2016). The observations confirmed the self-cleaning ability of labyrinth weirs, explained with the occurrence of complex vortices in the inlet key. Self-cleaning was correlated with the densimetric Froude number F_d (e.g., Gebhardt et al. 2018)

$$\mathsf{F}_d = \frac{U}{\sqrt{\frac{\rho_s - \rho}{\rho} g d_s}} \tag{1}$$

and started for around $\mathsf{F}_d > 1.1-1.4$ for a rectangular labyrinth weir. The sediments [0.7 mm $\le d_s \le$ 5.6 mm (Herbst 2016; Leitz 2016)] were washed out for $\mathsf{F}_d > 5$. Note that F_d was defined with the average upstream channel approach flow velocity U, the sediment ρ_s and water ρ densities, and the mean sediment diameter d_s.

Experimental Setup

The geometry of PKWs (Pralong et al. 2011) includes vertical height P, streamwise length B, parapet wall height R, side wall thickness T_s, and linear transverse width W. Subscript i refers to the inlet key, i.e., the key filled with water if the reservoir surface equals the PKW crest; and subscript o refers to the outlet key. These subscripts are used in the context of B, P, and W.

Systematic experimental tests were performed in a straight research channel at the Laboratory of Hydraulic Constructions (LCH) of the Ecole Polytechnique Fédérale de Lausanne (EPFL) (Noseda 2017). The channel was horizontal, 4.5 m long, and $W = 0.665$ m wide for PKW Configuration A (Table 1), and $W = 0.630$ m wide for Configurations B and C. The channel was thus slightly larger than the PKWs for the latter two configurations. A 0.3-m-thick planar and movable sediment bed was provided in the channel, up to the PKW mounted at the channel end (Fig. 1). The length of the considered sediment bed was approximately 4.0 m, plus a 0.5-m-long sediment ramp at the channel inlet, which was hydrodynamically shaped to avoid a model effect at the inlet. Submergence of the PKW from the tailwater was excluded because of a high vertical drop. Three different A-Type PKW configurations were tested (Table 1). These geometries covered a certain geometrical range in order to generalize the results.

A fine quartz sand and a quartz gravel were used as sediments (Fig. 2), both noncohesive and with rounded grains. The granulometry of the sand was specified as $d_{10} = 1.5$ mm, $d_{50} = 1.8$ mm, and $d_{90} = 2.5$ mm. The uniformity coefficient was $\sigma = (d_{90}/d_{10}) = 1.33$, the angle of repose was 35°, and the density was 2,603 kg/m^3. The granulometry of the gravel included $d_{10} = 5.6$ mm, $d_{50} = 6.9$ mm, and $d_{90} = 8.0$ mm. Consequently, $\sigma = 1.20$, the angle of repose was 43°, and the density was 2.650 kg/m^3. Normalizing characteristic sediment dimensions with the vertical PKW height P resulted in $0.01 \le d_{50}/P \le 0.08$ and $0.02 \le d_{90}/P \le 0.10$. Applying the d_{50}/P range to typical prototype PKWs with 3.0 m $\le P \le$ 5.0 m (Laugier et al. 2013; Ho Ta Khanh et al. 2011) indicated that the results are valid from gravel riverbeds up to armored layers composed of cobbles (excluding torrents, of course). These cobbles constitute the weight limit for the passage over a weir.

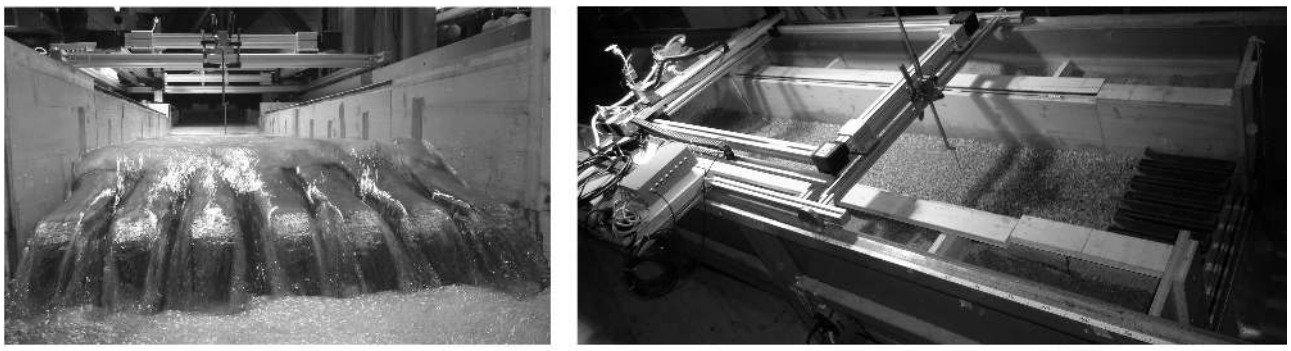

(a) (b)

Fig. 1. Physical model with automatic trolley, viewed from (a) downstream; and (b) side.

J. Hydraul. Eng., 2019, 145(8): 04019029

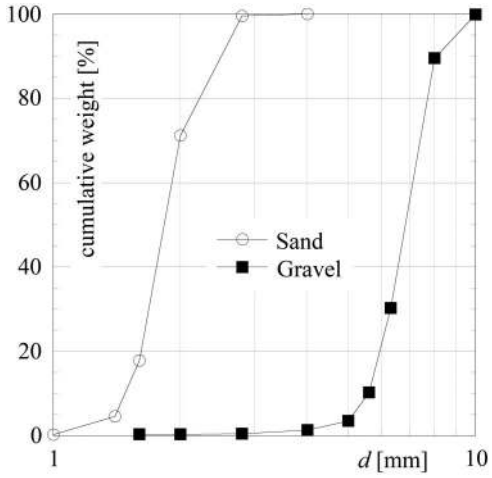

Fig. 2. Grading curves of tested sediments.

Before starting a test series, the sediments were inserted horizontally into the channel over its entire length. The vertical extension of the sediments reached initially to the crest level of the PKW [Fig. 3(a), up to $z = 0$ m in Fig. 4]. Even the PKW inlet keys were filled with sediments. Then the pumps were started and a small discharge [typically $Q = 0.015$ m^3/s (Table 2)] was provided. The latter was maintained constant for the necessary duration until an equilibrium scour with a steady riverbed occurred upstream of the PKW. The bathymetry was then scanned with an automatic trolley (described subsequently). Thereafter, the eroded riverbed was subjected to an increased discharge and eroded further. This procedure was repeated up to high discharges generating a pronounced erosion combined with a low riverbed (Fig. 3). No sediments were supplied during the tests so that the erosion developed under clear-water conditions.

Table 2 shows the test program, including 23 experiments. The discharge Q was held constant during a test (stationary flow). For the different tests, it was systematically varied as $0.015 \le Q \le 0.090$ m^3/s. More precisely, the maximum tested discharge was 0.060 m^3/s for the sand, and 0.090 m^3/s for the gravel to provoke a more pronounced erosion. The discharge spectrum corresponded to a range of $0.15 \le H/P \le 1.44$. Upstream channel Froude numbers $\mathsf{F} = U/(gh)^{0.5}$ in the range $0.44 \le \mathsf{F} \le 0.97$ occurred for the quasi-equilibrium bathymetry (Table 2). The discharge was measured with a magnetic inductive flow meter (±0.5% at full span). Water levels were measured along the channel centerline from the PKW up to the beginning of the channel using a point gauge up to ±1 mm [Fig. 1(a)]. The PKW head H was computed on the basis of the average water level measurements between $0.2 \text{ m} < x < 2.0$ m minus the PKW crest elevation (Fig. 4), including the kinematic head. The sediment bed bathymetry was measured with a laser distance sensor (Baumer Electric AG, Frauenfeld, Switzerland, OADM 13I7480/S35A] fixed on an automatic trolley [Fig. 1(b)] up to ±1 mm vertically. A validation of the horizontal laser position provided by the trolley indicated a precision of 1 mm. The measured grid covered a surface of 2.00 m along the channel, starting at the PKW axis, times a width of 0.40 m transversally. The point spacing of the grid was 20 mm, so 2,142 bathymetric points were measured per test. Preliminary calibration tests indicated that the erosion process developed as a function of the streamwise coordinate x only [one-dimensional (1D)-phenomena], whereas the transverse variation was negligible. The transverse profiles were thus averaged to one single elevation per longitudinal point.

Scale effects in terms of the rating curve were presumably small, because the tests included $0.023 \text{ m} \le H \le 0.138$ m. Pfister et al. (2013a) recommend $H > 0.010$–0.015 m to avoid errors above 5%. Scale effects related to the erosion process were also small because the minimum sand grain size of $d_{10} = 1.5$ mm exceeded the limit value of 1.0 mm mentioned by Pagliara et al. (2006), and $d_{50} = 1.8$ mm is larger than 1.5 mm, as recommended by Novak et al. (2010).

Preliminary Tests

Evolution of Erosion in Time

Erosion is a time-dependent process, even under stationary flow. Nevertheless, a quasi-equilibrium bathymetry is achieved for a sufficiently long flow duration. A first preliminary measurement series (called EQ in Table 2) was conducted to study the effect of flow duration on the evolution of the riverbed bathymetry, under otherwise unchanged conditions. The sediments were first placed to generate a horizontal bed at $z = 0$ m and the pumps were subsequently started. After a cumulative flow duration of 1, 2 (1 + 1),

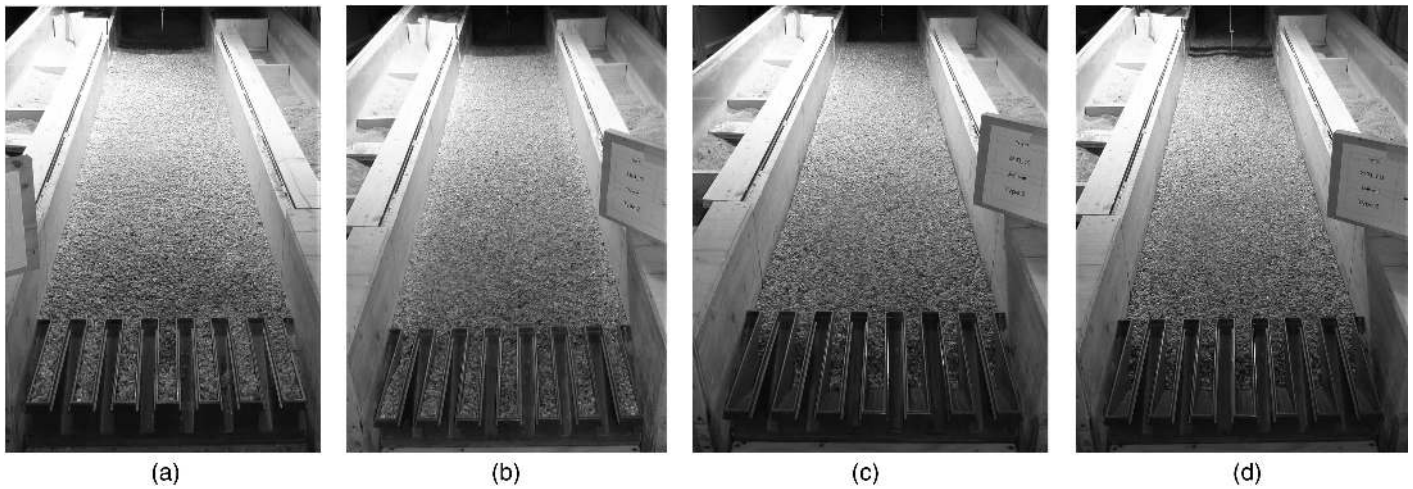

Fig. 3. Progressive riverbed erosion of Series 2 (Table 2): (a) initial condition with sediments up to PKW crest; (b) after Test 7 ($Q = 0.03$ m^3/s); (c) after Test 9 ($Q = 0.06$ m^3/s); and (d) after Test 11 ($Q = 0.09$ m^3/s).

J. Hydraul. Eng., 2019, 145(8): 04019029

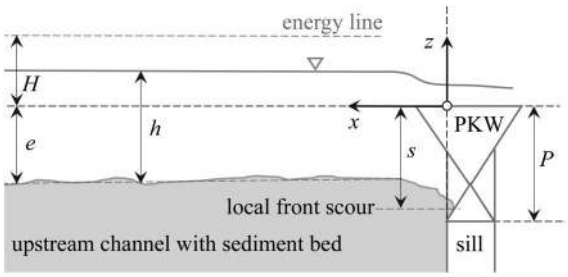

Fig. 4. Definition sketch of streamwise parameters near the PKW.

4 (1 + 1 + 2), 8 (1 + 1 + 2 + 4), and 16 (1 + 1 + 2 + 4 + 8) h [for series EQ (Table 2)], the water levels were measured and, consequently, the discharge was interrupted to record the riverbed bathymetry.

Fig. 5 shows the sediment bed as well as the water levels as measured after the mentioned cumulative flow durations. The bathymetries were essentially similar for a cumulative duration of 8 and 16 h. Even the cumulative duration of 4 h gave reliable erosions in the far field, but had small differences near the PKW. The riverbed bathymetry after a test duration of 16 h was on average 5 mm below that of 4 h and 2 mm below that of 8 h test duration. These differences occurred due to the discharge start after the previous test. Considering the eroded volumes and setting a duration of 16 h as the final condition, 88% was removed after 2 h, 95% after 4 h, and 98% after 8 h. It thus seemed reasonable to conduct tests of 4 h durations, and 6 h for the first test of a series for which erosion was observed. Table 2 lists durations of the individual tests, and not cumulative durations of the series. The water levels hardly varied, because they were essentially related to the rating curve. They seemed uninfluenced by the upstream erosion.

Gebhardt et al. (2018) suggested a test duration of 1.5 h to achieve quasi-equilibrium conditions for their model setup, and Jüstrich et al. (2016) also identified 1.5 h as adequate. However, both investigated local scour, whereas the present model with bed erosion reacted more slowly.

Modified Rating Curve due to High Upstream Sediment Level

The head H induced by the PKW affects the upstream channel flow depth h (Fig. 4). It is therefore essential to know the rating curve (H versus Q) for nonnegligible approach flow velocities U induced by high riverbeds. Such conditions were tested in a second preliminary measurement series (Table 3). To cover extreme scenarios, a fixed horizontal bed (formwork plate with polished smooth surface) was installed at $e/P = 0$ [$z = 0$ m (Fig. 6)], $e/P = 0.5$, and $e/P = 1$ for PKW Configurations A and B along the entire channel, also covering the inlet keys of the PKW.

Discharges up to $Q = 0.100$ m^3/s were supplied ($H/P \leq 1.44$). The upstream flow depth h was measured along the channel centerline, serving also for the determination of the PKW head H (Fig. 4). The data were compared with those of Pfister et al. (2013b) for a reservoir approach ($e/P \gg 1$), Venetz (2014) for channel approach flow with $1.53 \leq e/P \leq 3.68$, and Jüstrich et al. (2016) for a reservoir approach. Furthermore, two supplementary rating curves are provided: (1) critical flow (subscript C) as $H_C = 1.5(q^2/g)^{1/3}$ with $q = Q/W$, and (2) sharp-crested weir flow (subscript S) also with W as $Q_S = 0.42W(2gH_S^3)^{1/2}$. All mentioned data are compared in Fig. 7. The following issues are visible:

- tests with a fixed horizontal bed (Pfister, Jüstrich, Venetz, and $e/P = 0$, 0.5, and 1 present) indicated a modified rating curve if $e/P < 1$;

Table 2. Erosion test program in model dimensions

Series	Test number	Individual test duration (h)	Start sediment elevation	PKW configuration (Table 1)	Sediment type	Discharge, Q (m^3/s)	Channel Froude number F
EQ	1a	1	Crest	A	Sand	0.045	0.64
EQ	1b	1 (Cumulative 2)	Test 1a	A	Sand	0.045	0.56
EQ	1c	2 (Cumulative 4)	Test 1b	A	Sand	0.045	0.52
EQ	1d	4 (Cumulative 8)	Test 1c	A	Sand	0.045	0.50
EQ	1e	8 (Cumulative 16)	Test 1d	A	Sand	0.045	0.48
1	2	6	Crest	A	Sand	0.015	0.66
1	3	4	Test 2	A	Sand	0.030	0.51
1	4	4	Test 3	A	Sand	0.045	0.46
1	5	4	Test 4	A	Sand	0.060	0.44
2	6	1	Crest	A	Gravel	0.015	0.63
2	7	6	Test 6	A	Gravel	0.030	0.92
2	8	4	Test 7	A	Gravel	0.045	0.96
2	9	4	Test 8	A	Gravel	0.060	0.86
2	10	4	Test 9	A	Gravel	0.075	0.79
2	11	4	Test 10	A	Gravel	0.090	0.73
3	12	0.5	Crest	B	Gravel	0.015	0.72
3	13	6	Test 12	B	Gravel	0.030	0.89
3	14	4	Test 13	B	Gravel	0.045	0.97
3	15	4	Test 14	B	Gravel	0.060	0.90
3	16	4	Test 15	B	Gravel	0.075	0.78
3	17	4	Test 16	B	Gravel	0.090	0.71
4	18	6	Crest	B	Sand	0.015	0.63
4	19	4	Test 18	B	Sand	0.030	0.52
4	20	4	Test 19	B	Sand	0.045	0.48
4	21	4	Test 20	B	Sand	0.060	0.45
5	22	6	Crest	C	Sand	0.045	0.45
6	23	6	Crest	C	Gravel	0.045	0.87

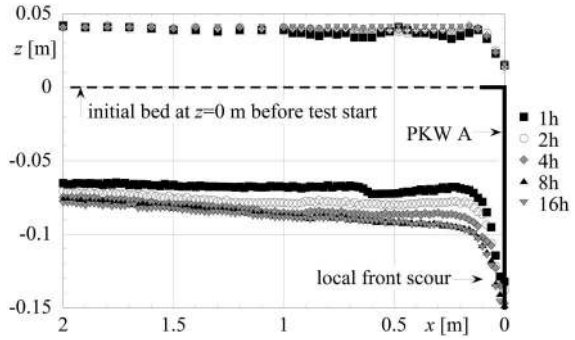

Fig. 5. Longitudinal bathymetry as measured after various cumulative flow durations [negative z-values, Series EQ (Table 2)] below and corresponding water surface profiles on top (positive z-values).

Table 3. Rating curve test program in model dimensions

Q	PKW Configuration A			PKW Configuration B		
(m^3/s)	$e/P = 1$	$e/P = 0.5$	$e/P = 0$	$e/P = 1$	$e/P = 0.5$	$e/P = 0$
0.005	—	—	—	—	—	X
0.010	X	X	X	X	X	X
0.015	X	X	X	X	—	X
0.020	X	X	X	X	X	X
0.025	—	—	—	X	—	—
0.030	X	X	X	X	X	X
0.035	—	—	—	X	X	—
0.040	X	X	X	X	X	X
0.045	—	—	—	X	—	—
0.050	X	X	X	X	X	X
0.055	—	—	—	X	—	—
0.060	X	X	X	X	X	X
0.065	—	—	—	X	—	—
0.070	X	X	—	X	X	X
0.075	—	—	—	X	—	—
0.080	X	X	—	X	X	—
0.085	—	—	—	X	—	—
0.090	X	—	—	X	—	—
0.095	—	—	—	X	—	—
0.100	—	—	—	X	—	—

- tests with a mobile bed (denoted by hollow crosses, for Series 1 and 2) indicated a modified rating curve as long as approximately $e/P < 0.7$;
- the rating curve was unaffected if $e/P \geq 1$ for all tests; and
- the condition $e/P = 0$ approached critical flow and sharp-crested weir flow (i.e., $H \approx H_C$ and $H \approx H_S$ respectively).

Accordingly, the rating curve was unaffected by the upstream channel flow as long as $e/P \geq 1$, at least within the tested discharge limit of $H/P \leq 1.44$. For mobile beds, the influence was less pronounced, probably because of the local upstream front-scour at the PKW (Figs. 5 and 9) shaped by the complex upstream weir flow. The erosion depth e of the sediment tests refers to the average bed elevation along the channel, excluding the local upstream PKW front-scour s (Fig. 4).

The nonaffected PKW rating curve ($e/P > 1$) was empirically defined by Leite Ribeiro et al. (2012) considering a dimensionless discharge increase ratio r formulated as

$$r = \frac{Q}{Q_S} = 1 + 0.24\delta \quad \text{for } e/P \geq 1 \tag{2}$$

where Q = PKW discharge; Q_S = sharp-crested weir discharge considering W as transverse width and serving as reference value; and

Fig. 6. PKW Configuration A (Table 1) and upstream channel with a fixed horizontal bed at elevation $e/P = 0$ equal to $z = 0$ m (Fig. 4).

δ = normalization coefficient [Eq. (3)]. Again, the ratio r considers sharp-crested weir flow as lower limit. This observation was also made in Fig. 7 for $e/P = 0$, where the PKW rating curve approached sharp-crested weir conditions (i.e., H_S). Thus, the rating curves of the sharp-crested weir and of the PKW nearly collapse if $e/P = 0$. The normalization coefficient δ is given by Leite Ribeiro et al. (2012) as

$$\delta = \left(\frac{(L - W)P_i}{WH}\right)^{0.9} \tag{3}$$

The values r and δ from Eqs. (2) and (3) were computed for the present data ($e/P \leq 1$), based on the measured PKW discharge Q, the computed reference sharp-crested weir discharge Q_S, and the (implicitly) measured PKW head H. The ratio r derived from the measurements was divided by $\zeta = 0.73$ for PKW Configuration A and by $\zeta = 0.95$ for PKW Configuration B to account for distal weir ends (Leite Ribeiro et al. 2012), so that the data can directly be compared to Eq. (2).

Fig. 8(a) shows r versus δ for PKW Configurations A and B and for a fixed horizontal channel bed. All data for $e/P = 1$ followed the trend line [Eq. (2)] provided by Leite Ribeiro et al. (2012) standing for not affected flow. Data with $e/P = 0.5$ followed a trend line with half inclination, so the inclination term 0.24δ in Eq. (2) was multiplied by 0.5. Finally, the data with $e/P = 0$ resulted in $r \approx 1$, indicating that sharp-crested weir flow was approached. The inclination term of the trend line was then zero. These observations lead to the conclusion that the term e/P can directly be included in Eq. (2) to modify the inclination term of the trend line. Eq. 2 then becomes

$$r = 1 + 0.24\delta\left(\frac{e}{P}\right)$$
$$\text{for } H/P \leq 1.44,\ 0 \leq e/P \leq 1, \text{ and a fixed upstream bed} \tag{4}$$

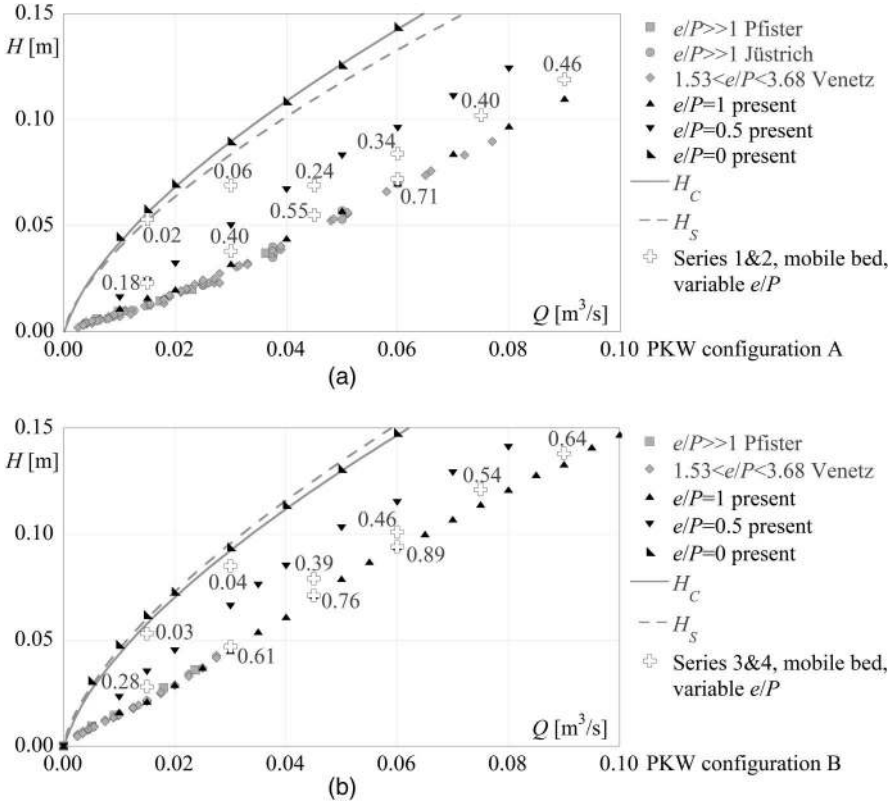

Fig. 7. Rating curves: PKWs (a) Configuration A; and (b) Configuration B.

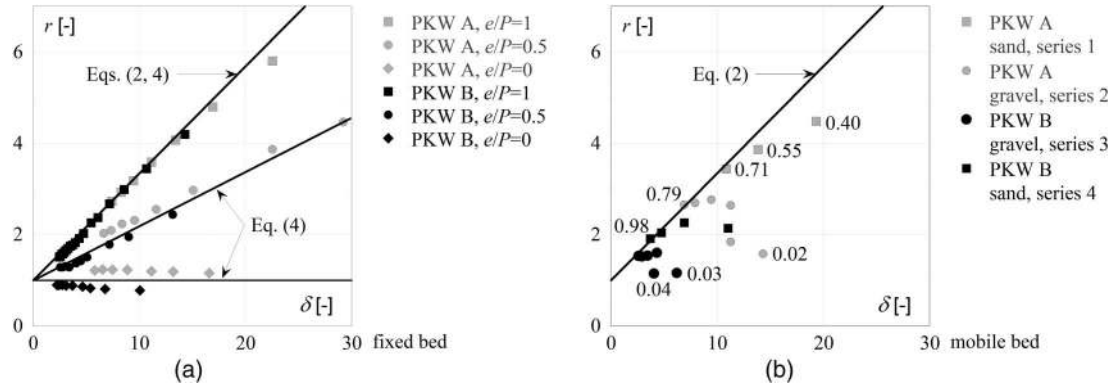

Fig. 8. Normalized PKW rating curves r versus δ for (a) fixed horizontal upstream bed including $e/P = 1$, 0.5, and 0; and (b) mobile sediment bed (labels indicate selected e/P).

Fig. 8(b) shows r versus δ for PKW Configurations A and B, and for a mobile sediment bed. The same trend as described for Fig. 8(a) is visible, but less pronounced. Values of e/P [labelled values in Fig. 8(b)] between 1 and roughly 0.7 were hardly affected, whereas smaller values of e/P had significant decreases of r. The effect of e/P was thus different from that with a fixed bed, so Eq. (4) was adapted for the mobile bed to

$$r = 1 + 0.24\delta\left(\frac{e}{P}\right)^{0.75}$$

$$\text{for } H/P \le 1.44,\ 0 \le e/P \le 1, \text{ and a mobile upstream bed} \quad (5)$$

Fig. 9 compares measured r values with computed r values [Eqs. (4) and (5)], including data with a fixed and a mobile bed. The coefficient of determination for all data (preliminary rating curve tests and erosion tests) was $R^2 = 0.97$.

Sediment Passage over PKW

General Observations

Fig. 10(a) shows the bathymetries and surface profiles for Series 2 (Table 2) as a representative example. The smallest tested discharge $Q = 0.015$ m^3/s (Test 6) initiated no systematic sediment erosion and was thus only maintained for 1 h. Higher discharges generated erosion, first near the PKW [$Q = 0.030$ m^3/s (Test 7)] and then along the entire channel [$Q \ge 0.045$ m^3/s (Tests 8–11)]. The sediment bed lowered over the entire surface with increasing discharge,

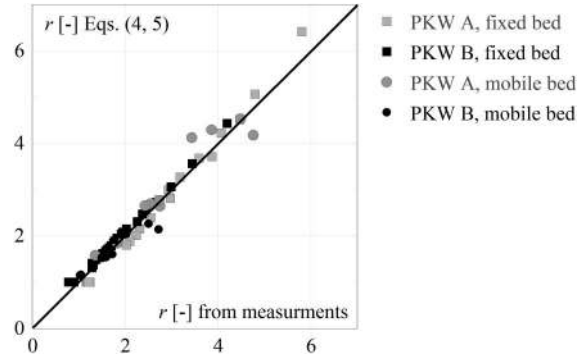

Fig. 9. Measured and computed r values.

indicating a global erosion tendency without deposits. Accordingly, all activated sediments passed over the PKW.

The erosion depths e of all series are summarized in Fig. 10(b) as a function of Q. As expected, the erosion depth e increased with discharge (i.e., the upstream equilibrium bed elevation decreased), because the shear stress augmented in parallel. Sand allowed for deeper erosion than gravel, as anticipated. The flow depths h along the channel (Fig. 4) were identical for the same discharge and sediment type, whereas the erosion depths e slightly varied due to the different rating curve per PKW configuration. This observation motivated (1) the analysis of the modified rating curve as presented previously, and (2) relating h (instead of e) to the erosion features in the channel.

Sediment Transport

The bed erosion along the channel was primary related to the channel flow and the sediment characteristics, and only secondary to the PKW. The flow depth h measured in the channel under quasi-equilibrium conditions could be predicted with sediment transport formulas. For the Van Rjin (1984a, b) (index V) approach, the measured flow depth h collapsed with h_V predicted for the channel sediment transport regime [Fig. 11(a), coefficient of determination $R^2 = 0.96$]. Similarly, the channel flow velocity U derived from flow depth measurement approached the prediction U_H following Hjulström (1935) (index H) for erosion onset [Fig. 11(b), gray range $d_{50} - d_{90}$]. Finally, the densimetric Froude numbers resulted in $\mathsf{F}_d \geq 2.7$ for the sand and $\mathsf{F}_d \geq 1.3$ for the gravel if d_{50} was selected. Again, for the test in which sediment transport occurred on the bed, these sediments also passed over the PKW. Comparing these values with those of Gebhardt et al. (2018) for rectangular labyrinth weirs and the start of self-cleaning ($\mathsf{F}_d \geq 1.1-1.4$)

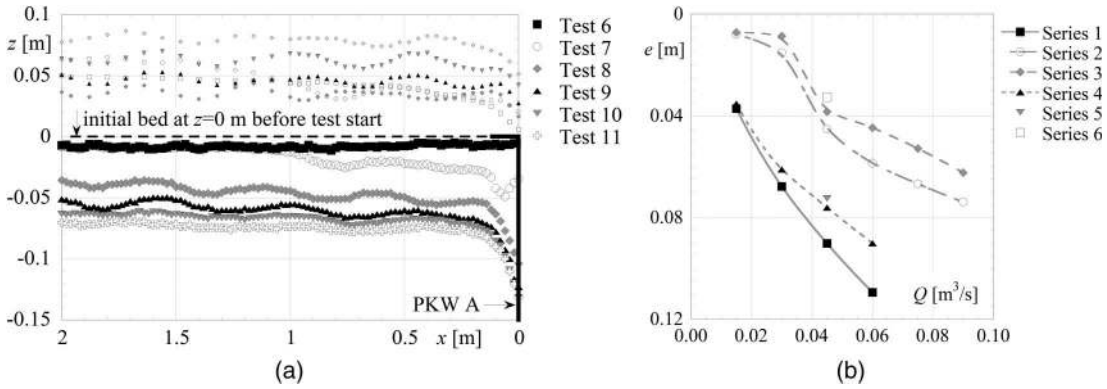

Fig. 10. (a) Longitudinal bathymetry and surface profiles for Series 2 (Table 2); and (b) averaged erosion depths e versus discharge Q for all tested series (Table 2).

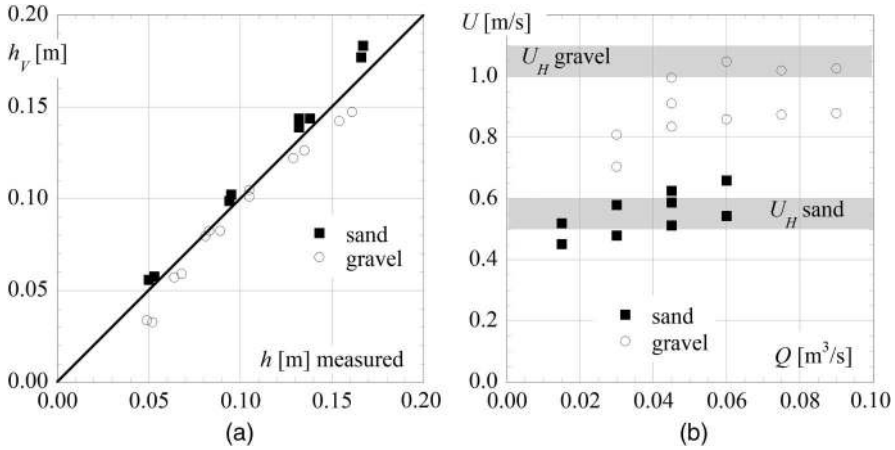

Fig. 11. (a) Measured flow depth h and value predicted based on Van Rjin h_V (1984a, b) for sediment transport; and (b) flow velocities U derived from flow depth measurements compared with erosion onset velocity U_H (shaded area) following Hjulström (1935).

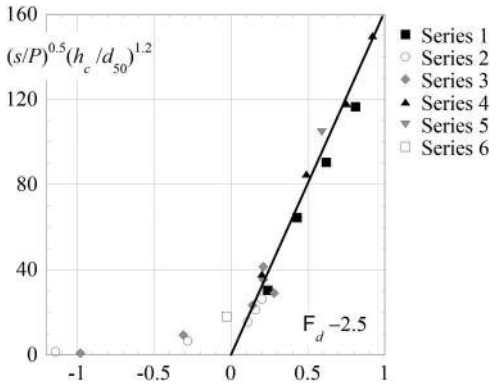

Fig. 12. Normalized front-scour depth s versus densimetric Froude number F_d.

indicated that the PKWs were operated in the self-cleaning mode herein. Gebhardt et al. (2018) observed completely clean (sediment-free) labyrinth weir inlet keys for $F_d > 5$, whereas the present study for PKWs showed that clean inlet keys occur if $F_d > 2.7$. This is not surprising, because PKWs provide a ramp as part of their structure to the sediments, whereas this ramp first has to be produced by the sediments themselves for labyrinth weirs.

It was concluded that the erosion of the sediment bed is only related to the channel conditions, and not to the PKW (unsubmerged operation). This suggests, as mentioned in the Introduction, that the passage of noncohesive sediment over a PKW was fully assured for all conditions tested in this study, proving the efficient self-cleaning capacity of PKW.

Upstream Front-Scour

The maximum local front-scour depth s (Fig. 4) was measured and normalized with the PKW height P as s/P, as well as with h_c/d_{50}. Plotting the normalized maximum front-scour depth against F_d indicated that noteworthy ($s/P > 0.5$) scouring at the PKW front occurred for roughly $F_d > 2.5$. Shifting F_d with that offset value resulted in the data in Fig. 12. The normalized front-scour depth is related to $(F_d - 2.5)$ as

$$\sqrt{\frac{|s|}{P}} \cdot \left(\frac{h_c}{d_{50}}\right)^{1.2} = 160 \cdot (F_d - 2.5) \quad \text{for } 2.5 \le F_d \le 3.5 \qquad (6)$$

The coefficient of determination was $R^2 = 0.95$ for the data with $2.5 \le F_d \le 3.5$ (positive values in Fig. 12). Effectively, a minor front-scouring process began at around $F_d > 2.0$, and amplified for $F_d \ge 2.5$. Again, the densimetric Froude number is the driving parameter to describe the interaction between sediments and weir. The local front-scour can exceed the PKW height P. Herein, a maximum value of $s/P = -1.54$ was observed for Tests 17 and 21.

Conclusions

The following observations are based upon the model tests conducted herein:

- A fixed bed inhibits the creation of a local upstream PKW front-scour s (Fig. 4), whereas a mobile bed allows for the generation of a local PKW front-scour. The resulting bathymetry with a mobile bed and a front-scour is more efficient in terms of the discharge rating curve.
- The normalized PKW rating curve proposed by Leite Ribeiro et al. (2012) can be adapted to account for high fixed or mobile beds, becoming hydraulically relevant if $e/P < 1$ (Fig. 4). The term e/P is included in Eq. (2) from Leite Ribeiro et al. (2012), so Eq. (4) results for a fixed bed and Eq. (5) for a mobile bed of sands and gravels.
- The global riverbed erosion (i.e., the upstream equilibrium bed level) was independent of the PKW features in the present tests. The erosion process occurred up to the erosion-transport condition suggested, for instance, by Hjulström (1935) and Van Rjin (1984a, b). Consequently, all sediments eroded and transported along the channel passed over the PKW for the tested setups.
- The riverbed erosion depth was $e = h + U^2/2g - H$ (Fig. 4). The flow depth h and the kinematic head $U^2/2g$ resulted from the sediment erosion-transport criterion along the channel. The PKW head H follows from Eqs. (3) and (5).
- Globally, sediment passage over the PKW was observed for all tests, indicating that a densimetric Froude number [as defined in Eq. (1)] of $F_d > 1.3$ was sufficient to allow for sediment passage over the tested PKWs. The inlet keys were partially filled with sediments for approximately $F_d = 1.3$. The inlet keys were clean (free of sediments) as soon as $F_d > 1.7$.
- A local scour developed at the upstream PKW front, reaching farther down than the mobile bed ($s \ge e$). This scour is important for the rating curve. The rating curve is less efficient if the front-scour generation is prevented, for instance, by placing riprap (resulting in a fixed bed).
- A significant upstream front-scour s occurs for $F_d > 2.5$. It can exceed $P(s > P)$ for fine sediments and high discharges. The depth s can be estimated with Eq. (6).
- The present study suggests that PKWs are more efficient in terms of their sediment passage capacity than are labyrinth weirs.
- The behavior of a live-bed was not tested herein, only clear-water conditions. One can speculate that the flow type in the channel corresponds to the transport regime instead of to the transport-erosion-onset regime, leading to a similar or a slightly higher sediment bed.
- We considered free overfall conditions, whereas in a river environment a PKW submergence can occur.

Acknowledgments

The authors thank Cédric Bron, lead technician at LCH, for his support during the model setup and operation.

Notation

The following symbols are used in this paper:

B = streamwise PKW length (m);
B_b = PKW base length (m);
d = sediment grain diameter (m);
e = erosion depth (upstream equilibrium bed level below crest) (m);
F = upstream channel Froude number;
F_d = densimetric Froude number;
g = acceleration due to gravity (m/s^2);
H = upstream PKW head (m);
H_C = upstream critical head (m);
H_S = upstream sharp-crested weir head (m);
h = flow depth on bed (m);
L = developed PKW crest length (m);
P = vertical PKW height (m);
Q = discharge (m^3/s);

R = coefficient of determination;
R = PKW parapet wall height (m);
r = discharge increase ratio;
s = upstream PKW front-scour (m);
T_S = PKW side wall thickness (m);
U = upstream channel velocity (m/s);
W = transverse width (m);
W_u = transverse width per cycle (m);
x = horizontal and counter-streamwise coordinate starting at the PKW (m);
z = vertical coordinate starting at the PKW crest (m);
δ = normalization coefficient;
ζ = coefficient for distal weir ends;
ρ = density (kg/m^3); and
σ = sediment uniformity coefficient.

Subscripts

C = critical flow;
H = sediment transport inception, following Hjulström;
i = inlet key;
o = outlet key;
S = sharp-crested weir;
s = sediment; and
V = sediment transport inception, following van Rjin.

References

Belzner, F., J. Merkel, M. Gebhardt, and C. Thorenz. 2017. "Piano key and labyrinth weirs at German waterways: Recent and future research of the BAW." In *Labyrinth and piano key weirs III*, 167–174. Leiden, Netherlands: CRC Press.

Belzner, F., J. Merkel, U. Pfrommer, M. Gebhardt, and C. Thorenz. 2016. "Piano-Key-Wehre und Labyrinth-Wehre unter den Randbedingungen einer Bundeswasserstrasse." *Wasserwirtschaft* 5 (106): 37–42.

Cassidy, J. J., C. A. Gardner, and R. T. Peacock. 1985. "Boardman labyrinth—Crest spillway." *J. Hydraul. Eng.* 111 (3): 398–416. https://doi.org/10.1061/(ASCE)0733-9429(1985)111:3(398).

Dabling, M. R., and B. P. Tullis. 2012. "Piano key weir submergence in channel applications." *J. Hydraul. Eng.* 138 (7): 661–666. https://doi.org/10.1061/(ASCE)HY.1943-7900.0000563.

Falvey, H. 2003. *Hydraulic design of Labyrinth weirs*. Reston, VA: ASCE.

Gebhardt, M., J. Herbst, J. Merkel, and F. Belzner. 2018. "Sedimentation at labyrinth weirs—An experimental study of the self-cleaning process." *J. Hydraul. Res.* 1–12. https://doi.org/10.1080/00221686.2018.1494053.

Guan, D., B. Melville, and H. Friedrich. 2015. "Live-bed scour at submerged weirs." *J. Hydraul. Eng.* 141 (2): 04014071. https://doi.org/10.1061/(ASCE)HY.1943-7900.0000954.

Herbst, J. 2016. "Hydraulische Untersuchungen an Labyrinth-Wehren zur Durchgängigkeit von Treibgut, Geschiebe und Eis." Master thesis, Karlsruhe Institute of Technology, and Bundesanstalt für Wasserbau.

Herbst, J., M. Gebhardt, J. Merkel, F. Belzner, and C. Thorenz. 2018. "Sediment transport over labyrinth weirs." In *Proc., 7th IAHR Int. Symp. Hydraulic Structures*. Madrid, Spain: International Association for Hydro-Environment Engineering and Research.

Hjulström, F. 1935. "Studies of the morphological activity of rivers as illustrated by the River Fyris." Ph.D. thesis, Geological Institute, Univ. of Uppsala.

Ho Ta Khanh, M., C. H. Truong, and T. H. Nguyen. 2011. "Main results of the P.K. weir model tests in Vietnam (2004–2010)." In *Labyrinth and piano key weirs*, 191–198. Leiden, Netherlands: CRC Press.

Jüstrich, S., M. Pfister, and A. J. Schleiss. 2016. "Mobile riverbed scour downstream of a piano key weir." *J. Hydraul. Eng.* 142 (11): 04016043. https://doi.org/10.1061/(ASCE)HY.1943-7900.0001189.

Lauchlan, C. 2004. "Experimental investigation of bed-load and suspended-load transport over weirs." *J. Hydraul. Res.* 42 (5): 551–558. https://doi.org/10.1080/00221686.2004.9641224.

Laugier, F., J. Vermeulen, and V. Lefebvre. 2013. "Overview of piano key weirs experience developed at EDF during the past few years." In *Labyrinth and piano key weirs II*, 213–226. Leiden, Netherlands: CRC Press.

Leite Ribeiro, M., M. Pfister, A. J. Schleiss, and J.-L. Boillat. 2012. "Hydraulic design of A-type piano key weirs." *J. Hydraul. Res.* 50 (4): 400–408. https://doi.org/10.1080/00221686.2012.695041.

Leitz, A. 2016. "Sedimenttransport bei Labyrinth-Wehren." Bachelor thesis, Institut, für Hydromechanik, Karlsruhe Institute of Technology KIT, and Bundesanstalt für Wasserbau BAW.

Machiels, O., M. Pirotton, P. Archambeau, B. Dewals, and S. Erpicum. 2014. "Experimental parametric study and design of piano key weirs." *J. Hydraul. Res.* 52 (3): 326–335. https://doi.org/10.1080/00221686.2013.875070.

Noseda, M. 2017. "Upstream erosion at piano key weirs." M.Sc. thesis, Laboratory of Hydraulic Constructions, Ecole Polytechnique Fédérale de Lausanne.

Novak, P., V. Guinot, A. Jeffrey, and E. D. Reeve. 2010. *Hydraulic modeling: An introduction*. London: Spon Press.

Oertel, M. 2018. "Piano key weir research: State-of-the-art and future challenges." In *Proc., 7th IAHR Int. Symp. Hydraulic Structures*. Madrid, Spain: International Association for Hydro-Environment Engineering and Research.

Ota, K., S. Sato, R. Arai, and H. Nakagawa. 2017. "Local scour upstream of a slit weir: Ordinary differential equation-based model under steady and unsteady flow conditions." *J. Hydraul. Eng.* 143 (1): 04016073. https://doi.org/10.1061/(ASCE)HY.1943-7900.0001215.

Pagliara, S., W. H. Hager, and H.-E. Minor. 2006. "Hydraulics of plane plunge pool scour." *J. Hydraul. Eng.* 132 (5): 450–461. https://doi.org/10.1061/(ASCE)0733-9429(2006)132:5(450).

Pfister, M., E. Battisacco, G. De Cesare, and A. J. Schleiss. 2013a. "Scale effects related to the rating curve of cylindrically crested piano key weirs." In *Labyrinth and piano key weirs II*, 73–82. Leiden, Netherlands: CRC Press.

Pfister, M., D. Capobianco, B. Tullis, and A. J. Schleiss. 2013b. "Debris blocking sensitivity of piano key weirs under reservoir type approach flow." *J. Hydraul. Eng.* 139 (11): 1134–1141. https://doi.org/10.1061/(ASCE)HY.1943-7900.0000780.

Phillips, M. A., and E. J. Lesleighter. 2013. "Piano Key weir spillway: Upgrade option for a major dam." In *Labyrinth and piano key weirs II*, 159–168. Leiden, Netherlands: CRC Press.

Pralong, J., J. Vermeulen, B. Blancher, F. Laugier, S. Erpicum, O. Machiels, M. Pirotton, J. L. Boillat, M. Leite Ribeiro, and A. J. Schleiss. 2011. "A naming convention for the piano key weirs geometrical parameters." In *Labyrinth and piano key weirs*, 271–278. Leiden, Netherlands: CRC Press.

Sharma, N., and H. Tiwari. 2013. "Experimental study on vertical velocity and submergence depth near Piano Key weir." In *Labyrinth and piano key weirs II*, 93–100. Leiden, Netherlands: CRC Press.

Van Rjin, L. C. 1984a. "Sediment transport. Part I: Bed load transport." *J. Hydraul. Eng.* 110 (10): 1431–1456. https://doi.org/10.1061/(ASCE)0733-9429(1984)110:10(1431).

Van Rjin, L. C. 1984b. "Sediment transport. Part II: Suspended load transport." *J. Hydraul. Eng.* 110 (11): 1613–1641. https://doi.org/10.1061/(ASCE)0733-9429(1984)110:11(1613).

Venetz, P. 2014. "Einfluss von Schwemmholz auf die Abflusscharakteristik von Klaviertasten-Wehren." M.Sc. thesis, Laboratory of Hydraulic Constructions, Ecole Polytechnique Fédérale de Lausanne.